ATMOSPHERIC AND OCEANIC SCIENCE LETTERS, 2012, VOL. 5, NO. 4, 301–305

The Interannual Variations of Summer Precipitation in the Northern Indian Ocean Associated with ENSO

YANG Ya-Li[1,2], DU Yan[2], WU Yan-Ling[1,2], HUANG Gang[3], and ZHANG Yong-Sheng[4]

[1] *Graduate University of Chinese Academy of Sciences, Beijing 100049, China*
[2] *State Key Laboratory of Tropical Oceanography, South China Sea Institute of Oceanology, Chinese Academy of Sciences, Guangzhou 510301, China*
[3] *Key Laboratory of Regional Climate-Environment Research for Temperate East Asia (RCE-TEA), Institute of Atmospheric Physics, Chinese Academy of Sciences, Beijing 100029, China*
[4] *Earth System Science Interdisciplinary Center (ESSIC), University of Maryland, USA*

Received 29 March 2012; revised 18 May 2012; accepted 28 May 2012; published 16 July 2012

Abstract Using rainfall data from the Global Precipitation Climatology Project (GPCP), NOAA extended reconstruction sea surface temperature (ERSST), and NCEP/NCAR reanalysis, this study investigates the interannual variation of summer rainfall southwest of the Indian Peninsula and the northeastern Bay of Bengal associated with ENSO. The composite study indicates a decreased summer rainfall southwest of the Indian Peninsula and an increase in the northeastern Bay of Bengal during the developing phase, but vice versa during the decay phase of El Niño. Further regression analysis demonstrates that abnormal rainfall in the above two regions is controlled by different mechanisms. Southwest of the Indian Peninsula, the precipitation anomaly is related to local convection and water vapor flux in the decay phase of El Niño. The anomalous cyclone circulation at the lower troposphere helps strengthen rainfall. In the northeastern Bay of Bengal, the anomalous rainfall depends on the strength of the Indian southwest summer monsoon (ISSM). A strong/weak ISSM in the developing/decay phase of El Niño can bring more/less water vapor to strengthen/weaken the local summer precipitation.

Keywords: Indian summer monsoon, ENSO, interannual variability

Citation: Yang, Y.-L., Y. Du, Y.-L. Wu, et al., 2012: The interannual variations of summer precipitation in the northern Indian Ocean associated with ENSO, *Atmos. Oceanic Sci. Lett.*, **5**, 301–305.

1 Introduction

The Indian summer monsoon has an important impact on the social and economic activities of residents within its zone of influence. Previous studies found that large-scale air-sea interactions, such as the El Niño-Southern Oscillation (ENSO) and the Indian Ocean Dipole (IOD), are essential factors contributing to variations in precipitation (Saji et al., 1999; Webster et al., 1999). El Niño alters atmospheric circulation and affects the climate remotely via atmospheric wave adjustments by changing the atmospheric convection over the central-to-eastern equatorial Pacific (Klein et al., 1999; Alexander et al., 2002). Numerous studies have investigated the relationships between El Niño and regional climate in the tropical Indian Ocean (e.g., Lau and Nath, 2000; Xie et al., 2002). Many of these studies investigated the impacts of the IOD on the climate of the Indian Ocean and neighboring regions (e.g., Hastenrath, 2002; Ashok et al., 2003; Annamalai and Murtugudde, 2004). Saji et al. (1999) and Webster et al. (1999) found a high correlation between the IOD and East Africa precipitation. During the positive IOD, a warming SST emerges at the Western Indian Ocean (WIO) and a cooling SST emerges at the Eastern Indian Ocean (EIO), bringing a positive rainfall anomaly in the WIO and a negative rainfall anomaly in the EIO (Saji and Yamagata, 2003).

In the Southwestern Indian Ocean (SWIO), a previous study indicated that the SST warms starting in early spring in the decay phase of El Niño (Wu et al., 2008; Schott et al., 2009). Due to the Wind-Evaporation-Sea Surface Temperature (WES) feedback, the southward SST gradients stimulate an antisymmetric pattern of atmospheric anomalies, with northeasterly and northwesterly wind anomalies north and south of the equator, respectively (Xie and Philander, 1994; Kawamura et al., 2001; Wu et al., 2008). The antisymmetric wind pattern anchored by the SWIO warming persists until early summer in the decay phase of El Niño. Subsequently, the antisymmetric wind field pattern brings two effects: a warming SST over the North Indian Ocean (NIO) and a weakening of the summer Indian monsoon, producing anomalous summer precipitation (Du et al., 2009; Parthasarathy et al., 1991). Izumo et al. (2008) used observations and an advanced coupled atmosphere-ocean general circulation model to show that the northeasterly anomaly can weaken the upwelling along the Somalia-Oman coast to warm the SST over the western Arabian Sea. The increasing SST along the Somalia-Oman coast enhances the moisture transport toward India and strengthens the monsoon rainfall during the decay phase of El Niño.

The present study investigates the summer rainfall in the Northern Indian Ocean (NIO) associated with ENSO events. Our results show that there is an opposite response of summer rainfall anomalies to the developing and decaying phases of El Niño. We propose a mechanism different from that of Izumo et al. (2008) to explain the variation of precipitation southwest of the Indian Penin-

Corresponding author: DU Yan, duyan@scsio.ac.cn

sula. The rest of the paper is organized as follows: Section 2 describes the data and methods; Section 3 illustrates the characteristics of the summer precipitation over NIO and gives the results of composite and regression analyses; and Section 4 presents a summary and discussion of this study.

2 Data and methods

The Global Precipitation Climatology Project (GPCP) version 2.2 monthly combined precipitation with a resolution of 2.5°×2.5° was used (Adler et al., 2003). The extended reconstructed sea surface temperature (ERSST) by the National Oceanic and Atmospheric Administration (NOAA) is available on a 2.5° grid (Smith et al., 2008). The National Centers for Environmental Prediction-National Center for Atmospheric Research (NCEP-NCAR) atmospheric reanalysis (Kalnay et al., 1996) used here includes 850-hPa wind and specific humidity with a resolution of 2.5°×2.5°. The data span January 1979 to December 2010 to consider the impacts of El Niño on the tropical Indian Ocean climate, which exhibited a dramatic change in the mid-1970s (Xie et al., 2010).

To highlight the signal of the interannual variability, all the data were filtered with a 4- to 84-month band-pass filter, and their long trends were removed. The empirical orthogonal function (EOF) analysis, composite and regression methods were used to analyze the interannual variations of the NIO summer precipitation. In addition, the developing and decay years of ENSO were designated by 0 and 1.

3 Results

3.1 Precipitation differences in the two regions

Due to its complexity, the Indian monsoon rainfall has received much attention. Figure 1a shows that there are two maximum centers of the root mean square (RMS) of the summer (June-July-August, JJA) precipitation anomaly over the Northern Indian Ocean (NIO). One center is located southwest of the Indian Peninsula (SWIP), with a peak at the west coast of the Indian Peninsula. This peak indicates the orographic effect from the Western Ghats mountain range (Izumo et al., 2008) and mountain-anchored precipitation (Xie et al., 2006). The other center is located the northeastern Bay of Bengal (NEBB), and its large value extends from northwest to southeast, covering a wide area.

Figure 1b shows the first EOF mode of the NIO summer (JJA) rainfall variability. The EOF emerges as a dipole-like mode, with a weak decrease over the Indian Peninsula and neighboring ocean to its west and the southern Bay of Bengal. A major increase is shown in the NEBB, extending from northwest to southeast, which is similar to the result of Fig. 1a. The principal components (PCs, Fig. 1c) of the first EOF mode indicate an obvious interannual variability. In addition, in strong ENSO years, the PCs and Niño-3.4 index have the same variation trend.

To further investigate the rainfall pattern, we selected two relatively small domains: the SWIP and the NEBB

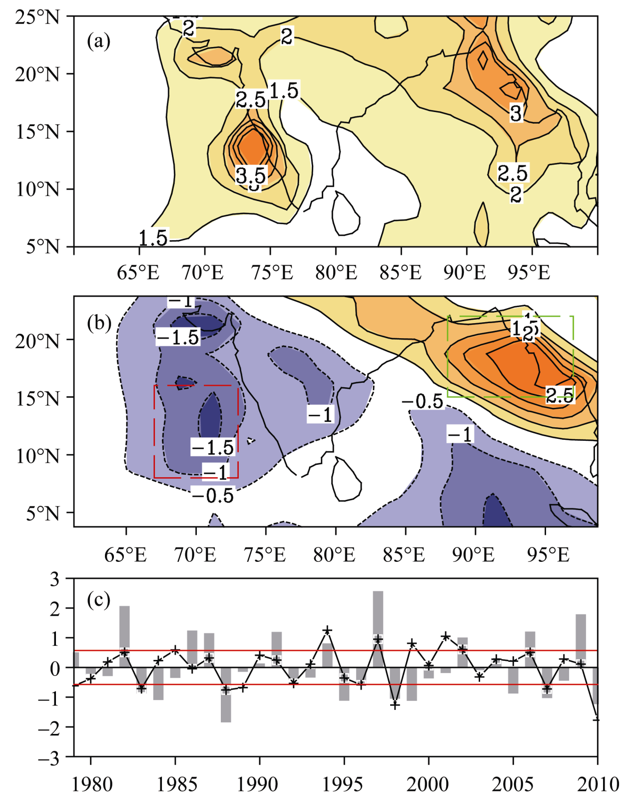

Figure 1 (a) RMS of summer (JJA) rainfall anomaly; (b) First EOF mode of summer rainfall anomaly, the red and green boxes show the regions of the SWIP (8–16°N, 67–73°E) and the NEBB (15–22°N, 88–97°E), respectively; (c) The principal components (PCs, black line) of the First EOF mode and the 32-year time series for the NDJ(0) Niño-3.4 index (shaded gray, °C), red line denotes the range of the standard deviation of the PCs.

(Fig. 1b, red and green boxes). The designated SWIP area (Fig. 1b, red box) does not include the west coast of the Indian Peninsula to avoid the orographic effect caused by the mountain range. A 32-year time series of JJA rainfall for the SWIP and the NEBB and the November-December-January (NDJ)(0) Niño-3.4 index were used to study the relationships between them (Fig. 2). The result indicates an opposite relationship between the SWIP and the NEBB summer rainfall anomalies, with a correlation coefficient –0.47. More rainfall in the SWIP usually corresponds to less rainfall in the NEBB. The NEBB rainfall is positively correlated to the Niño-3.4 index, with a correlation coefficient 0.42; for the SWIP rainfall, it is –0.47. All the correlation coefficients pass the 95% confidence level. The time series of JJA rainfall confirm the result from the EOF analysis and, thus, the solid relationships between the summer rainfall over the NIO and ENSO events.

3.2 Composite results

To demonstrate the anomalous atmospheric circulation and the NIO conditions, a composite is made based on the following standards: the recognized ENSO year (Meyers et al., 2007) and its PCs are larger than one standard deviation. We chose 1982, 1994, 1997, and 2006 as positive cases and 1983, 1988, 1998, 2007, and 2010 as negative cases. Figure 3 shows the composited anomalies of precipitation, 850-hPa wind, and SST in JJA. The left panel (positive cases) presents the summer JJA(0) in the ENSO developing phase, while the right panel (negative cases) presents the JJA(1) in the ENSO decaying phase.

Over the Arabian Sea and the Bay of Bengal, the wind anomalies are strong westerlies in JJA(0) and easterlies in JJA(1), consistent with former analyses (Xie et al., 2009; Du et al., 2009). The SST warms significantly over the Arabian Sea and the Bay of Bengal in JJA(1). This warming is attributed to the positive shortwave radiation flux and positive atmospheric forcing component of latent heat flux (AtF-L), the latter associated with anomalous easterlies (Du et al., 2009). An anticyclonic circulation covers the SWIP in JJA(0) and depresses the deep convection, leading to a negative rainfall anomaly. In JJA(1), however, a cyclone circulation anomaly occupies over the region and enhances convection, resulting in more precipitation over the SWIP. In the Arabian Sea, the enhanced westerly wind bring more water vapor to the NEBB and increases rainfall in JJA(0). In a reverse situation, an anomalous easterly wind weaken the climatological monsoonal wind and decreases the local precipitation.

3.3 The regression

This section presents results from regression and demonstrates how ENSO affects the rainfall over the region. Figure 4 shows the regression of rainfall, 850-hPa wind, and water vapor flux divergence on the NDJ(0) Niño-3.4 index. The results are consistent with the previous composite analysis (Fig. 3). The dipole-like mode of precipitation over the NIO are represented precisely. The anticyclonic circulation over the SWIP, the westerly anomalies over the NEBB at JJA(0), the cyclonic circulation over the SWIP and the easterly anomalies over the NEBB at JJA(1) are all seen in the regression results. The water vapor flux anomalies, with a divergence over the SWIP at JJA(0) and the NEBB at JJA(1) while converging over the NEBB at JJA(0) and the SWIP at JJA(1), are consistent with the precipitation anomalies. Overall, the wind and water vapor flux plays an essential role in the NIO

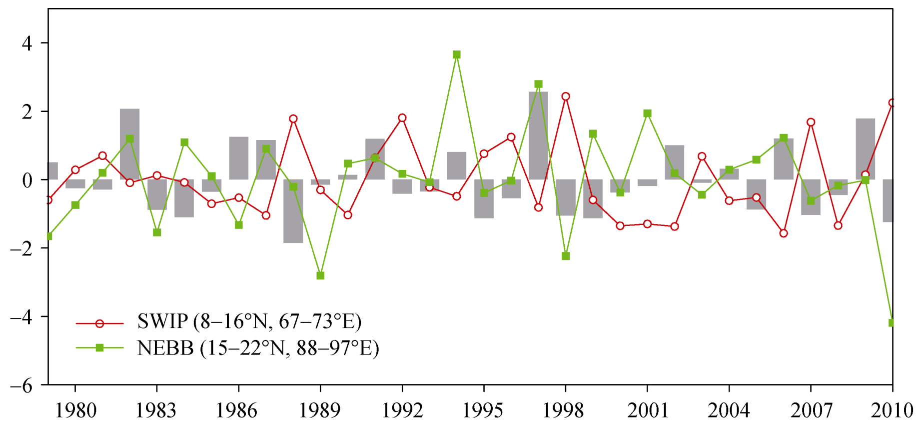

Figure 2 32-year time series of JJA rainfall for the SWIP (red line, mm d^{-1}), the NEBB (green line, mm d^{-1}), and the NDJ(0) Niño-3.4 index (gray shaded, °C).

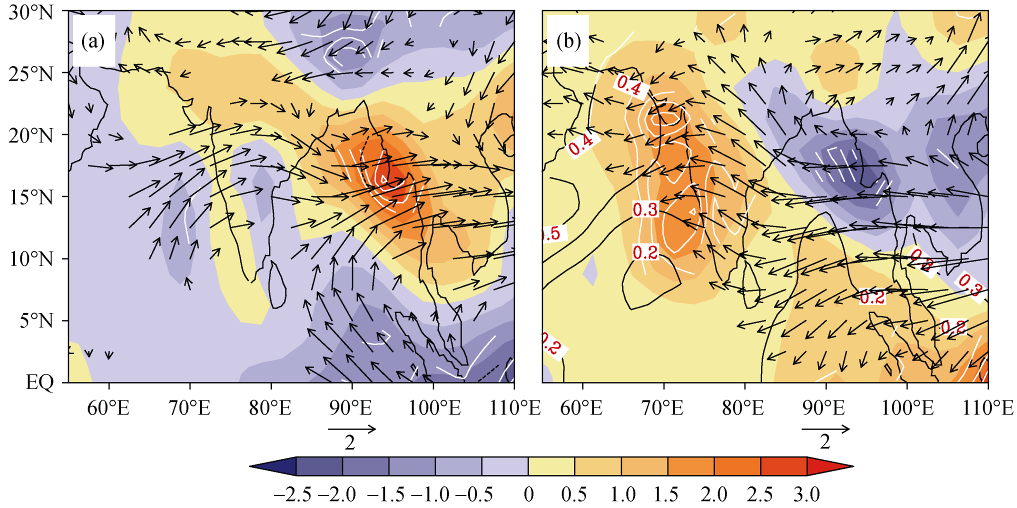

Figure 3 Composite of (a) positive and (b) negative cases of rainfall anomalies (shaded, mm d^{-1}; rainfall anomalies exceeding the 90% significance level are denoted with white contours), 850-hPa wind anomalies (vector, m s^{-1}; wind speed anomalies lower than a 90% significance level are masked out), and SSTA (contours, °C; SSTAs less than a 90% significance level are masked out).

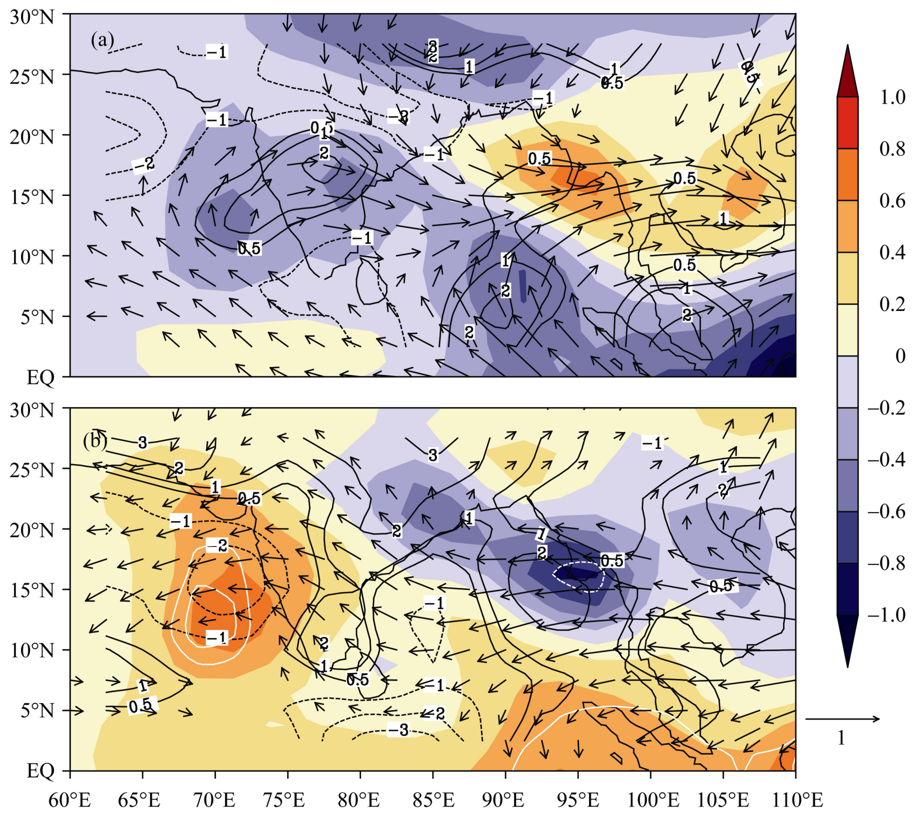

Figure 4 Regression on the NDJ(0) Niño-3.4 index for (a) JJA(0) and (b) JJA(1): rainfall (shaded, mm d^{-1}), 850-hPa water vapor flux divergence (contours, 10^{-5} kg m^{-1} s^{-1}), and 850-hPa wind anomalies (vector, m s^{-1}; wind speed anomalies less than 0.2 m s^{-1} have been masked out). The thin and thick white lines denote confidence levels over 90% and 95% of the correlation coefficients of JJA(1) rainfall correlated with the NDJ(0) Niño-3.4 index, respectively.

summer rainfall anomaly during ENSO events.

4 Summary and discussions

This study investigated the interannual variations of summer rainfall in the regions southwest of the Indian Peninsula (SWIP) and the northeastern Bay of Bengal (NBBB). Variations related to the atmospheric circulation associated with ENSO were found. Our primary analysis was based on EOF methods, composites, and regressions of summer rainfall referenced to the NDJ(0) Niño-3.4 SST index. During the summer of the developing phase of an El Niño event (JJA(0)), an anticyclonic anomaly covers the SWIP, which depresses the local convection and decreases the precipitation, while westerly anomalies bring more water vapor to the NEBB, increasing the summer rainfall over the region. However, the circulation condition reverses during the summer (JJA(1)) following El Niño, with a cyclonic circulation over the SWIP and easterly anomalies prevailing over the Bay of Bengal, resulting in strengthened rainfall over the SWIP and weakened rainfall over the NEBB. The local SST contributes to convection to some extent, but the convergence of the wind and rich water vapor transports are more important factors enriching the precipitation.

Xie et al. (2009) investigated the Indian Ocean capacitor effect on the Indo-Western Pacific climate during the summer following El Niño. With a correlation analysis between rainfall and NDJ(0) Niño-3.4, they found a positive correlation over the tropical Indian Ocean (TIO) but a weak correlation at the NEBB in summer following El Niño (JJA(1)). Their results suggested that the response of the NEBB rainfall to ENSO varies greatly from case to case. We double-check the correlation, as shown in Fig. 4b, and find that it is similar to that in Xie et al. (2009). Why do the EOF and regression illustrate a close relationship of rainfall with ENSO over the NEBB but the correlation does not? The high monsoonal variations, independent of ENSO, may be a reason. Different regional responses to the different climate regimes may be another reason. We leave this question open to further investigation in the future.

Acknowledgements. This work is supported by the National Basic Research Program of China (973 Program, 2010CB950302&2012 CB955603), the Knowledge Innovation Program of the Chinese Academy of Sciences (Grant No. XDA05090404), and the National Natural Science Foundation of China (41149908).

References

Adler, R. F., G. J. Huffman, A. Chang, et al., 2003: The version 2 Global Precipitation Climatology Project (GPCP) monthly precipitation analysis (1979–present), *J. Hydrometeor.*, **4**, 1147–1167.

Alexander, M. A., I. Bladé, M. Newman, et al., 2002: Theatmospheric bridge: The influence of ENSO teleconnections on air-sea interaction over the global oceans, *J. Climate*, **15**, 2205–2231.

Annamalai, H., and R. Murtugudde, 2004: Role of the Indian Ocean in regional climate varibility. Earth's climate: The ocean-atmosphere interaction, *Geophys. Monogr. Ser.*, **147**, 213–246.

Ashok, K., Z. Y. Guan, N. H. Saji, et al., 2003: Individual and combined influences of ENSO and the Indian Ocean dipole on the Indian summer monsoon, *J. Climate*, **17**, 3141–3155.

Du, Y., S.- P. Xie, G. Huang, et al., 2009: Role of air-sea interaction in the long persistence of El Niño-induced North Indian Ocean warming, *J. Climate*, **22**(8), 2023–2038.

Hastenrath, S., 2002: Dipoles, temperature gradients, and tropical climate anomalies, *Bull. Amer. Meteor. Soc.*, **83**, 735–738.

Izumo, T., C. B. Montégut, J.-J. Luo, et al., 2008: The role of the western Arabian sea upwelling in Indian monsoon rainfall variability, *J. Climate*, **21**, 5603–5623.

Kalnay, E., M. Kanamitsu, R. Kistler, et al., 1996: The NCEP/NCAR 40-year reanalysis project, *Bull. Amer. Meteor. Soc.*, **77**, 437–471.

Kawamura, R., T. Matsumura, and S. Iizuka, 2001: Role of equatorially asymmetric sea surface temperature anomalies in the Indian Ocean in the Asian summer monsoon and El Niño-Southern Oscillation coupling, *J. Geophys. Res.*, **106**, 4681–4693.

Klein, S. A., B. J. Soden, and N.-C. Lau, 1999: Remote sea surface variations during ENSO: Evidence for a tropical atmospheric bridge, *J. Climate*, **12**, 917–932.

Lau, N.-C., and M. J. Nath, 2000: Impact of ENSO on the variability of the Asian-Australian monsoons as simulated in GCM experiments, *J. Climate*, **13**, 4287–4309.

Meyers, G., P. McIntosh, L. Pigot, et al., 2007: The years of El Niño, La Niña, and interactions with the tropical Indian ocean, *J. Climate*, **20**, 2872–2880.

Parthasarathy, B., K. Rupa Kumar, and V. R. Deshpande, 1991: Indian summer monsoon rainfall and 200 mb meridional wind index: Application for long-range prediction, *Int. J. Climatol*., **11**, 165–176.

Saji, N. H., B. N. Goswami, P. N. Vinayachandran, et al., 1999: A dipole in the tropical Indian Ocean, *Nature*, **401**, 360–363.

Saji, N. H., and T. Yamagata, 2003: Possible impacts of Indian Ocean dipole mode events on global climate, *Climate Res.*, **25**, 151–169.

Schott, F. A., S.-P. Xie, and J. P. McCreary, 2009: Indian Ocean circulation and climate variability, *Rev. Geophys.*, **47**, RG1002, doi:10.1029/2007RG000245.

Smith, T. M., R. W. Reynolds, T. C. Peterson, et al., 2008: Improvements to NOAA's Historical Merged Land-Ocean Surface Temperature Analysis (1880–2006), *J. Climate*, **21**, 2283–2296.

Webster P. J., A. M. Moore, J. P. Loschnigg, et al., 1999: Coupled ocean-atmosphere dynamics in the Indian Ocean during 1997–98, *Nature*, **401**, 356–360.

Wu, R., B. P. Kirtman, and V. Krishnamurthy, 2008: An asymmetric mode of tropical Indian Ocean rainfall variability in boreal spring, *J. Geophys. Res*., **113**, D05104, doi:10.1029/2007JD009316.

Xie, S.-P., H. Annamalai, F. A. Schott, et al., 2002: Structure and mechanisms of South Indian Ocean climate variability, *J. Climate*, **15**, 864–878.

Xie, S.-P., Y. Du, G. Huang, et al., 2010: Decadal shift in El Niño influences on Indo-western Pacific and East Asian climate in the 1970s, *J. Climate*, **23**, 3352–3368.

Xie, S.-P., K. Hu, J. Hafner, et al., 2009: Indian Ocean capacitor effect on Indo-western Pacific climate during the summer following El Niño, *J. Climate*, **22**, 730–747.

Xie, S.-P., and S. G. H. Philander, 1994: A coupled ocean-atmosphere model of relevance to the ITCZ in the eastern Pacific, *Tellus A*, **46**, 340–350.

Xie, S.-P., H. Xu, N. H. Saji, et al., 2006: Role of narrow mountains in large-scale organization of Asian monsoon convection, *J. Climate*, **19**, 3420–3429.